Site-Directed Spin Labeling Electron Paramagnetic Resonance Study of the Calcium-Induced Structural Transition in the N-Domain of Human Cardiac Troponin C Complexed with Troponin I†

Shoji Ueki,‡ Motoyoshi Nakamura,‡ Tomotaka Komori,§ and Toshiaki Arata*,‡

Department of Biology, Graduate School of Science, Osaka University, Toyonaka, Osaka 560-0043, Japan, and Graduate School of Frontier Bioscience, Osaka University, Suita, Osaka 565-0871, Japan

Received September 2, 2004; Revised Manuscript Received October 25, 2004

ABSTRACT: Calcium-induced structural transition in the amino-terminal domain of troponin C (TnC) triggers skeletal and cardiac muscle contraction. The salient feature of this structural transition is the movement of the B and C helices, which is termed the "opening" of the N-domain. This movement exposes a hydrophobic region, allowing interaction with the regulatory domain of troponin I (TnI) as can be seen in the crystal structure of the troponin ternary complex [Takeda, S., Yamashita, A., Maeda, K., and Maeda, Y. (2003) *Nature 424*, 35−41]. In contrast to skeletal TnC, Ca^{2+}-binding site I (an EF-hand motif that consists of an A helix−loop−B helix motif) is inactive in cardiac TnC. The question arising from comparisons with skeletal TnC is how both helices move according to Ca^{2+} binding or interact with TnI in cardiac TnC. In this study, we examined the Ca^{2+}-induced movement of the B and C helices relative to the D helix in a cardiac TnC monomer state and TnC−TnI binary complex by means of site-directed spin labeling electron paramagnetic resonance (EPR). Doubly spin-labeled TnC mutants were prepared, and the spin−spin distances were estimated by analyzing dipolar interactions with the Fourier deconvolution method. An interspin distance of 18.4 Å was estimated for mutants spin labeled at G42C on the B helix and C84 on the D helix in a Mg^{2+}-saturated monomer state. The interspin distance between Q58C on the C helix and C84 on the D helix was estimated to be 18.3 Å under the same conditions. Distance changes were observed by the addition of Ca^{2+} ions and the formation of a complex with TnI. Our data indicated that the C helix moved away from the D helix in a distinct Ca^{2+}-dependent manner, while the B helix did not. A movement of the B helix by interaction with TnI was observed. Both Ca^{2+} and TnI were also shown to be essential for the full opening of the N-domain in cardiac TnC.

Skeletal and cardiac muscle contraction is regulated by a Ca^{2+}-dependent structural transition in the muscle thin filaments (*1*, *2*). The signals for this contraction, which is induced by variations in the Ca^{2+} concentration, are transferred through troponin (Tn)[1] on the thin filaments. Tn is composed of three distinct subunits, TnC, TnI, and TnT (*3*). TnC is a dumbbell-shaped molecule that consists of amino- and carboxy-terminal globular domains (N- and C-domains, respectively) connected by a central linker (*4*, *5*). TnC is a calmodulin superfamily molecule and binds Ca^{2+} ions at the EF-hand motifs. Binding of Ca^{2+} to the N-domain and the consequential structural transition in the N-domain are the first steps of the transition in thin filaments.

Skeletal TnC has two Ca^{2+}-binding sites (sites I and II) in the N-domain. Site I is an EF-hand motif that consists of an A helix−loop−B helix motif, and site II consists of a C helix−loop−D helix motif (the five helices in the N-domain are labeled as N and A−D). Ca^{2+} binding induces the movement of the B and C helices relative to other helices, and the hydrophobic region exposed by the movement interacts with the regulatory domain (residues 150−159) of TnI (*6*). Cardiac TnC, on the other hand, has only one Ca^{2+}-binding site (site II) with inactivation of site I due to an insertion (V28) and substitution (from D30 and D32 in skeletal TnC to L29 and A30, respectively, in cardiac TnC) at the EF-hand motif (*7*). Opening of the N-domain in cardiac TnC is thought to be different from that in skeletal TnC due to the lack of site I. NMR analysis (*8*) and a fluorescence resonance energy transfer (FRET) study (*9*) revealed that not only Ca^{2+} binding but also interaction with the regulatory domain of TnI is necessary for full opening of the N-domain of cardiac TnC. Recently, the crystal structure of a cardiac Tn ternary complex was reported (*10*), in which the N-domain of TnC was shown to have an open conformation. However, it is still unclear how the movement of each helix depends on Ca^{2+} binding and interaction with TnI.

In this study, we examined the Ca^{2+}-induced movement of the B and C helices relative to the D helix in a cardiac

† This work was supported by grants from the Special Coordination Funds of the Ministry of Education, Culture, Sports, Science and Technology, Japan.

* To whom correspondence should be addressed: Department of Biology, Graduate School of Science, Osaka University, Toyonaka, Osaka 560-0043, Japan. Telephone: +81-6-6850-5427. Fax: +81-6-6850-5441. E-mail: arata@bio.sci.osaka-u.ac.jp.

‡ Graduate School of Science, Osaka University.

§ Graduate School of Frontier Bioscience, Osaka University.

[1] Abbreviations: Tn, troponin; TnC, troponin C; TnI, troponin I; TnC(C84), TnC(C35S) mutant; TnC(G42C/C84), TnC(C35S/G42C) mutant; TnC(Q58C/C84), TnC(C35S/Q58C) mutant; SDSL, site-directed spin labeling; EPR, electron paramagnetic resonance; MTSL, (1-oxyl-2,2,5,5-tetramethylpyrrolidin-3-yl)methyl methanethiosulfonate.

10.1021/bi048110w CCC: $30.25
Published on Web 12/04/2004

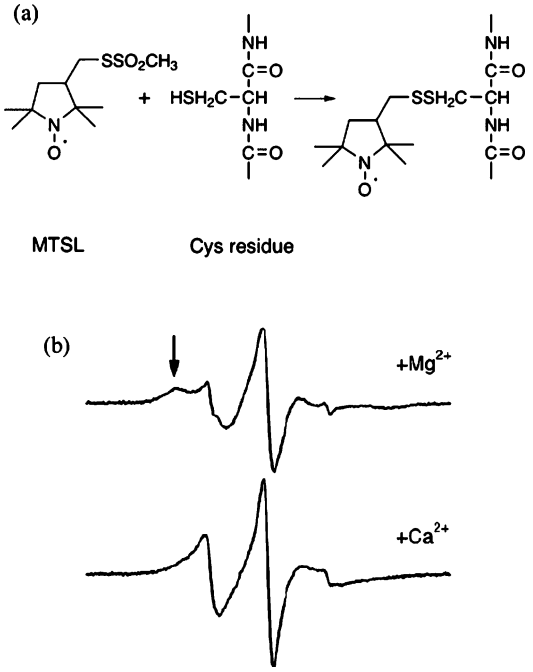

FIGURE 1: (a) Structure of the methanethiosulfonate spin-label and its reaction with a cysteine residue. (b) EPR spectra of the spin-labeled TnC(C84) monomer in a 30% sucrose solution at 25 °C. The mobility of the spin-label was increased by the addition of Ca^{2+} (arrow). The scan width is 100 G.

TnC monomer state and cardiac TnC−TnI binary complex by means of site-directed spin labeling (SDSL) electron paramagnetic resonance (EPR). EPR spectroscopy monitors the mobility and environment of spin-labels attached to the cysteine residue. If a spin-label is close to other spin-labels, and depending on the distance between them, the spectrum is affected by the dipole interaction. A methanethiosulfonate spin-label (MTSL, Figure 1a) was used as the probe in this study. We examined two TnC mutants, each containing two cysteine residues. In one case, the cysteine residues were present in the B and D helices, and in the other, they were present in the C and D helices. The spin-labels were covalently attached to the cysteine residues as shown in Figure 1a; the structure of the N-domain (*11*) and the spin-labeled positions are shown in Figure 2. The spin−spin distances were estimated by analyzing dipolar interactions using the Fourier deconvolution method (*12*).

EXPERIMENTAL PROCEDURES

Plasmids and Mutagenesis. Native human cardiac TnC and TnI genes were obtained from Y. Maeda (RIKEN HARIMA, Hyogo, Japan), and site-directed mutagenesis was performed as previously described (*13*). Native human cardiac TnC has two cysteine residues at positions 35 and 84. First, we prepared the C35S (C84) mutant as a template and then introduced a cysteine at G42 on the B helix [TnC(G42C/C84); mutants are represented by their cysteine positions] or Q58 on the C helix [TnC(Q58C/C84)] by mutagenesis. Substitution of the desired residues was confirmed by DNA sequence analyses.

Expression and Purification. TnC mutants were expressed and purified as previously described (*13*). Briefly, mutant plasmids were used to transform competent *Escherichia coli* BL21(DE3) pLysS. Protein production was induced by addition of 1 mM isopropyl β-thiogalactoside, and induction was allowed to proceed for 5 h. The cells were harvested by centrifugation, and then the cell pellet was suspended in a buffer solution containing 20 mM Tris and 1 mM EDTA (pH 7.5) and then sonicated. Ammonium sulfate (60% w/v) was added to the cell extract in the buffer, and the solution was centrifuged. The supernatant was then dialyzed, loaded onto a Q-Sepharose anion exchange column (Amersham, Piscataway, NJ) equilibrated with the same buffer, and eluted with a KCl gradient; protein purity was confirmed by SDS−PAGE. Protein concentrations were determined by the Bradford method (Bio-Rad, Hercules, CA) using BSA as the standard. Dithiothreitol (2 mM) was added to the protein solution, which was then stored at −60 °C.

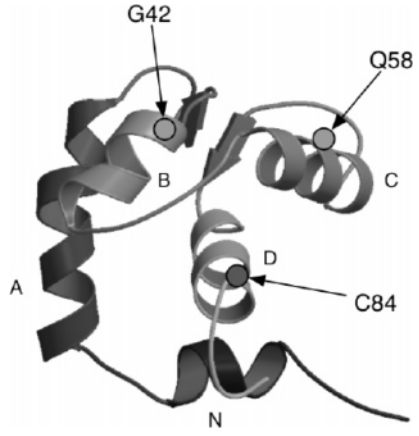

FIGURE 2: Structure of the N-domain of human cardiac TnC (PDB entry 1SPY). The spin labeling positions are shown in the structure. The five helices are labeled as N and A−D. This figure was generated with MOLSCRIPT (*36*) and Raster3D (*37*).

Human cardiac TnI was expressed using the same method for TnC. The cell pellet was suspended in a buffer solution containing 20 mM Tris, 8% sucrose, 5% Triton X-100, and 5 mM EDTA (pH 7.5), incubated at room temperature for 1 h, and then sonicated. The sonication procedure was repeated twice in the same buffer and once in 20 mM Tris and 1 mM EDTA (pH 7.5). The pellet was then resuspended in 6 M urea, 20 mM Tris, 0.1 M KCl, and 1 mM EDTA (pH 7.5) and centrifuged. The supernatant was applied to an SP-Sepharose cation exchange column (Amersham) equilibrated with the same buffer and eluted with a KCl gradient. Protein purity and concentration were determined as described above, and the protein was stored at −4 °C.

Spin Labeling of TnC Mutants. We used the (1-oxyl-2,2,5,5-tetramethylpyrrolidin-3-yl)methyl methanethiosulfonate spin-label (MTSL) purchased from Toronto Research Chemicals (North York, ON). After removal of DTT from the stock solution by application to a Sephadex G-25 desalting column (Amersham) equilibrated with a buffer containing 20 mM MOPS, 0.2 M KCl, and 1 mM EDTA (pH 7.1), TnC mutants were incubated with a 10-fold molar excess of MTSL. The reaction was allowed to proceed at room temperature for 1 h followed by the mixture being held overnight at −4 °C. Unattached MTSL was removed by application to a desalting column. The spin-label:protein ratios estimated by double integration of EPR spectra were ∼1.8:1 in both mutants.

Preparation of a TnC−TnI Binary Complex. A human cardiac TnC−TnI binary complex was prepared as described

by Dong et al. (*14*). Briefly, spin-labeled mutant TnC and TnI were mixed (1:3) in a buffer containing 20 mM MOPS, 6 M urea, 1 M KCl, and 50 mM Ca^{2+} (pH 7.1), and then stepwise dialyses were carried out to reduce the urea concentration. The final buffer solution contained 20 mM MOPS, 0.2 M KCl, 3 mM $MgCl_2$, and 1 mM EGTA (pH 7.0). TnI that did not form a complex with TnC was removed by centrifugation. The formation of a binary complex was confirmed by urea−PAGE (*15*).

Activity Assay. Protein activities of spin-labeled mutant TnC were assayed from the ATPase activities of TnC-substituted myofibrils. TnC extraction and substitution on a glycerinated rabbit psoas muscle were carried out as described by Moss (*16*). Ca^{2+}-dependent ATPase activities of the myofibrils were determined as described by Morimoto and Ohtsuki (*17*).

EPR Measurements and Spectral Analyses. EPR spectroscopy was performed on a Bruker ELEXSYS E500 spectrometer equipped with a dielectric resonator. Samples (10 μL) were loaded into 1.0 mm outside diameter capillaries sealed on both ends. EPR spectra were acquired using 1 G field modulation amplitude at 100 kHz and a 5 mW incident microwave power at 25 °C, or 0.1 mW at −100 °C. For the EPR measurements, a buffer containing 20 mM MOPS, 0.2 M KCl, and 3 mM $MgCl_2$ (pH 7.1) was used for the condition with Mg^{2+}, and 3 mM $CaCl_2$ was added to the buffer solution for the condition with Ca^{2+}. The protein concentrations in sample solutions were ∼60 μM for mutant TnC monomers and 30 μM for binary complexes.

The rotational correlation time for the TnC monomer was estimated to be 7 ns (*18*). To examine the motion of the spin-label relative to the protein, it is desirable to reduce the contribution of protein rotation. For this purpose, the spectra of the spin-labeled TnC monomer were recorded in 30% (w/v) sucrose. An addition of this amount of sucrose does not affect the rotational mobility of the side chain relative to the protein at room temperature (*19*).

Spin−spin interactions were analyzed from spectra recorded at −100 °C to remove the influence of side chain mobility on the spectra. Distances between the two spin-labels were estimated by the Fourier deconvolution method using a program kindly provided by Y. K. Shin (*20*). The EPR spectrum of a singly labeled TnC mutant at C84 was used as the noninteracting standard.

RESULTS

Previously, we reported increased spin-label mobility in the TnC(C84) mutant by addition of Ca^{2+} ions (*13*). The spectra are reproduced in Figure 1b for reference. This increased mobility was attributed to the Ca^{2+}-dependent removal of tertiary interactions from some residues on the B−C helix. In this study, the doubly spin-labeled mutant TnC(G42C/C84) was prepared for examination of Ca^{2+}-induced movement of the B helix in monomer and binary complexes, and mutant TnC(Q58C/C84) was used for the C helix.

Activity Assays of Mutant TnC. Ca^{2+}-dependent ATPase assays were carried out using spin-labeled mutant TnC-substituted myofibrils. The activity of the mutant TnC was assayed as the extent of ATPase inhibition without Ca^{2+} ions relative to the activity of native myofibrils. The spin-labeled TnC(G42C/C84) and TnC(Q58C/C84) were inhibited by 80 and 98% relative to the native myofibril, respectively (data not shown). A slight decrease in activity was observed in TnC(G42C/C84), and no malfunction was observed in TnC-(Q58C/C84).

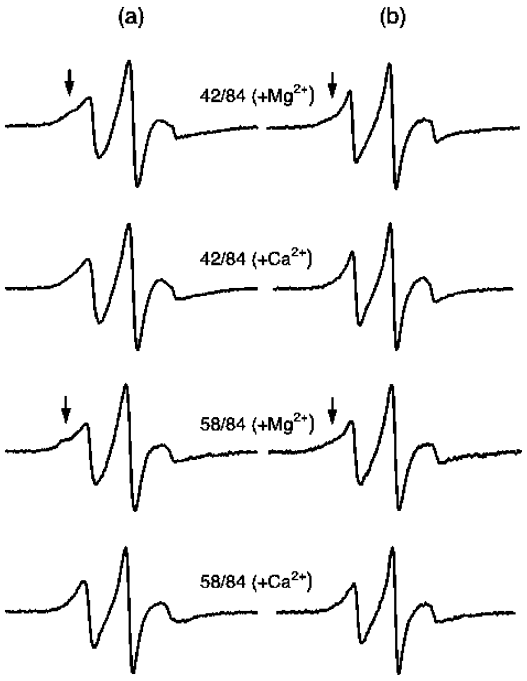

FIGURE 3: EPR spectra of spin-labeled TnC(G42C/C84) and TnC-(Q58C/C84) at 25 °C (a) in the monomer state and (b) in the TnC−TnI binary complex. The arrow indicates the slowly mobile component. The scan width is 100 G.

EPR Spectra at 25 °C. The EPR spectra of spin-labeled TnC(G42C/C84) and TnC(Q58C/C84) in a monomer state are shown in Figure 3a. All spectra were normalized to the same number of spins. The slowly mobile components (arrow) were reduced by the addition of Ca^{2+} ions in both mutants. These components are the contribution of the spin-label attached to the C84 position (*13*). The spectra show that the spin-labels at G42C and Q58C were more mobile than that at C84, and this indicates that these labels were more exposed to the solvent. In all spectra in a monomer state, the peak−peak line width of the central absorption was broadened relative to that of the singly labeled TnC(C84) (*13*). This broadening indicates that the spin−spin distances are less than 25 Å in all states (*21*). The EPR spectra of the TnC−TnI binary complex are shown in Figure 3b. The decreased slow components as a result of the Ca^{2+} ions were also observed in the binary complex, suggesting that the orientations of the spin-label side chains were not altered much by the formation of a binary complex.

EPR Spectra in the Frozen Solution and Estimation of Spin−Spin Distances. The EPR spectra at −100 °C are shown in Figure 4. The noninteracting singly labeled TnC-(C84) spectrum is also shown by the dotted lines. All spectra were normalized to the same number of spins. A decreased intensity relative to the noninteracting spectrum was observed in all spectra, indicating the existence of dipolar interaction. The spin−spin distances were estimated by the Fourier deconvolution method (*12*). In these estimations, we used one Gaussian function to fit the broadening function $M^*(\omega)$ in the Fourier space; this means that the mean distances were

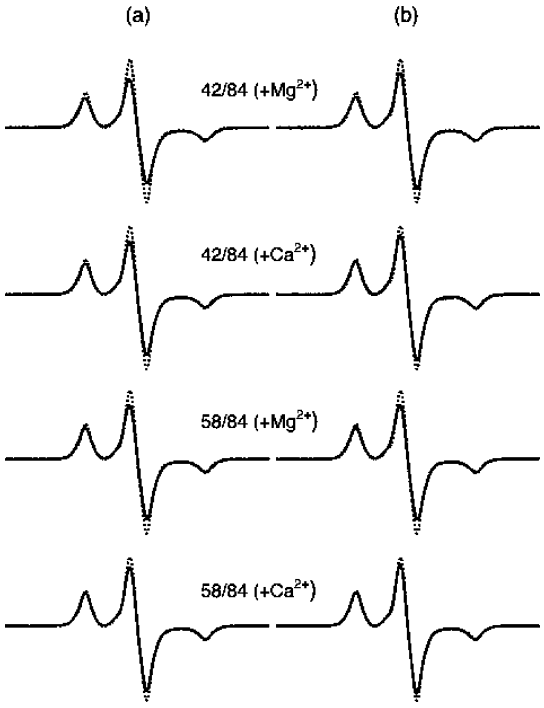

FIGURE 4: EPR spectra of spin-labeled TnC(G42C/C84) and TnC-(Q58C/C84) at −100 °C (a) in the monomer state and (b) in the TnC−TnI binary complex. The dotted line represents the non-interacting spectrum [spectrum of the spin-labeled TnC(C84) mutant]. The scan width is 160 G.

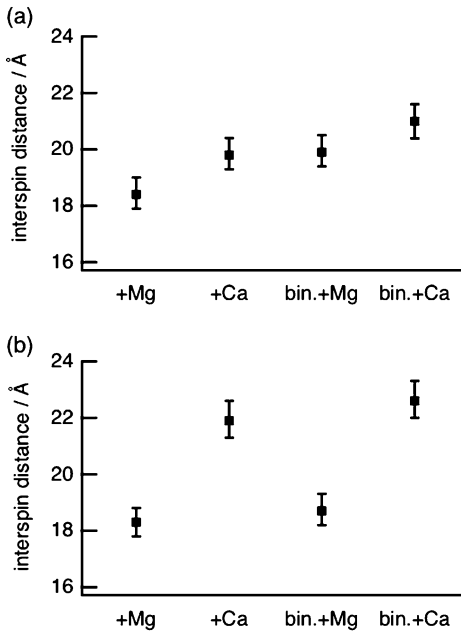

FIGURE 5: Interspin distances of spin-labeled (a) TnC(G42C/C84) and (b) TnC(Q58C/C84) in various states. The label bin. means the TnC−TnI binary complex. The bar indicates the standard error.

determined without considering the distance distribution. Monoradical contaminations estimated by the fitting were ~20% in most of the calculations. This is consistent with the labeling efficiency determined from the spectra (spin-label:protein ratio of 1.8:1) in the case of different reactivity between two labeling sites. Therefore, we estimated the final values of spin−spin distances in fixing the monoradical fraction to be 20%. Figure 5a shows the mean spin−spin distances of TnC(G42C/C84) with standard errors. The distance increased by 1.4 Å with the addition of Ca^{2+} ions in a monomer state, and this increase was almost the same in the binary complex with Mg^{2+}. A further increase was observed by the addition of Ca^{2+} ions in the binary complex. Figure 5b shows the distances of TnC(Q58C/C84). A distinct Ca^{2+}-induced increase in distance was observed in both the monomer and binary complex. Formation of a complex with TnI had little effect on the spin−spin distance in this spin-labeled mutant. The mean distances and distance changes relative to that of the Mg^{2+} monomer state are summarized in Table 1.

Table 1: Interspin Distances and Distance Changes of Doubly Spin-Labeled Mutant TnC[a]

mutant	state	mean distance (Å)	distance change[b] (Å)
G42/C84	with Mg^{2+}	18.4	−
	with Ca^{2+}	19.8	1.4
	bin. with Mg^{2+}	19.9	1.5
	bin. with Ca^{2+}	21.0	2.6
Q58/C84	with Mg^{2+}	18.3	−
	with Ca^{2+}	21.9	3.6
	bin. with Mg^{2+}	18.7	0.4
	bin. with Ca^{2+}	22.6	4.3

[a] The label bin. means the TnC−TnI binary complex. [b] The distance changes from the distance of the Mg^{2+} monomer state.

DISCUSSION

We examined the Ca^{2+}-dependent interspin distance changes of doubly spin-labeled TnC mutants in monomer and binary complexes. Native human cardiac TnC has two cysteine residues at positions 35 and 84. Since, in a previous study, spin labeling at C84 and mutation of C35 to serine had little effect on TnC activity (*13*), we used C84 on the D helix as the basis of the distance measurement. The B helix consists of T38−L48 (22). To examine the movement of the B helix relative to the D helix, we mutated G42 to cysteine, because this residue is exposed to solvent in the solution structure and its polarity resembles that of cysteine. Q58 was selected for the mutation on the C helix (P54−V64) using the same criteria that were used for G42.

We used the spectrum of a singly spin-labeled TnC(C84) mutant as the noninteracting spectrum for Fourier deconvolution calculations; however, strictly speaking, this is not a noninteracting spectrum of a doubly spin-labeled mutant. Because a noninteracting spectrum should be contain the information of spin-labels at both sites, a sum of two spin-labeled mutant spectra at each cysteine or a spectrum measured using a mixture containing the spin-label and a diamagnetic analogue produces a more ideal noninteracting spectrum of the double mutant (*23*). Under rigid solution conditions, the motions of spin-labels are frozen, and the circumstances of spin-labels become more identical. Therefore, the use of the spin-labeled TnC(C84) spectrum is a good approximation under rigid solution conditions, and it is thought not to alter the calculated relative change in distance.

In skeletal TnC, the B helix is a constituent of the EF-hand of Ca^{2+}-binding site I. The structures of two-Ca^{2+} (*4*) and four-Ca^{2+} skeletal TnC (*24*) indicate that the B helix moves away from the D helix in association with binding of Ca^{2+} to site I. In cardiac TnC, however, site I is inactive due to absence of several Ca^{2+}-binding residues. Our data suggest that the addition of Ca^{2+} induces little movement in

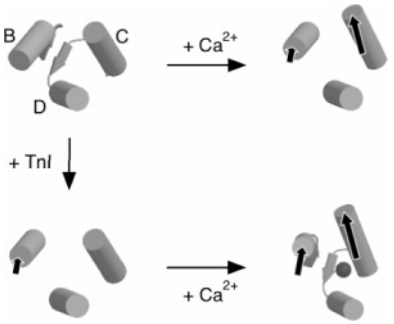

FIGURE 6: Schematic representation of the structural transition in the N-domain of human cardiac TnC. Only the B−D helices are drawn. The thick arrow represents the movement of the helix from the closed conformation (top left).

the B helix, while TnI is necessary for further movement. Ca^{2+}-induced movement of the B helix in a monomer state might be concomitant with movement of the C helix. A similar B helix opening was observed without Ca^{2+} binding to the N-domain in the binary complex. Phosphorylation of two serine residues (S23 and S24) in cardiac TnI causes a reduction in Ca^{2+} binding affinity in the N-domain of TnC (*25*−*27*), indicating that the N-terminal region of TnI interacts with the N-domain of TnC. Small angle neutron scattering (*28*) and cross-linking (*29*) studies suggest the existence of this interaction. Furthermore, NMR studies carried out by Rosevear and co-workers demonstrate that the unphosphorylated N-terminus of TnI binds to site I of TnC, and opens the N-domain of TnC (*30*−*32*). Trayer and co-workers also propose that the interaction stabilizes the open conformation of TnC (*33*). Therefore, we think that the B helix opening observed in the Mg^{2+} binary complex is the consequence of an interaction with the N-terminal region of TnI. This B helix movement might be a key mechanism for the regulation of Ca^{2+} affinity by the phosphorylation of N-terminus of cardiac troponin I.

The C helix, on the other hand, shows distinct Ca^{2+}-induced movement in both the monomer state and binary complex. This is a reasonable consequence because the C helix is a constituent of the EF-hand for site II, which is active in cardiac TnC. Reorientation of the Ca^{2+}-binding residues to form a pentagonal bipyramidal coordination around Ca^{2+} moves the C helix as observed (*34*), and formation of a binary complex with TnI had little effect on further opening of the C helix.

The closed structure of the N-domain has been determined in a Mg^{2+} monomer state by NMR (*11*), and the full open structure was also determined in a Ca^{2+} ternary complex by X-ray crystallography (*10*). These data suggest that the distance between the α-carbon of Q58 and that of C84 changes by ∼4.5 Å, according to the structural transition from closed to open. Our estimation of the change was 4.3 Å, which is consistent with the value obtained from the known structures of TnC. The distance changes between G42 and C84 were ∼4.2 Å according to the known structures and 2.6 Å according to our results, respectively. This difference might be related to the decreased activity (80%) of this mutant.

Considering the distance changes observed by Ca^{2+} binding and the interaction with TnI as an intermediate of the transition defined by known structures, the structural transition in the N-domain of TnC is summarized in Figure 6. Here, the top left represents the solution structure of the N-domain in a Mg^{2+} monomer state (*11*), and the bottom right represents the crystal structure in a Ca^{2+} ternary complex (*10*). Ca^{2+} binding moves the C helix to the almost full open conformation, and the B helix to some extent (top right). Interaction with TnI moves the B helix, but has almost no effect on the C helix (bottom left). Full opening is achieved by both Ca^{2+} binding and interaction with TnI. A mutagenesis study of two EF-hands in the N-domain of cardiac TnC revealed that activation of site I with inactivation of site II could not trigger contraction (*35*). According to this and our results, Ca^{2+}-induced movement of the C helix is mainly responsible for regulation of cardiac muscle contraction.

ACKNOWLEDGMENT

We thank Drs. Y. Maeda (RIKEN HARIMA) and S. Takeda (National Cardiovascular Center Research Institute, Suita, Japan) for providing us with the expression plasmids of human cardiac TnC and TnI, and for their helpful discussions.

REFERENCES

1. Ebashi, S., and Endo, M. (1968) Calcium ion and muscle contraction, *Prog. Biophys. Mol. Biol. 18*, 123−183.
2. Ebashi, S., Endo, M., and Ohtsuki, I. (1969) Control of muscle contraction, *Q. Rev. Biophys. 2*, 351−384.
3. Ohtsuki, I., Maruyama, K., and Ebashi, S. (1986) Regulatory and cytoskeletal proteins of vertebrate skeletal muscle, *Adv. Protein Chem. 38*, 1−67.
4. Herzberg, O., and James, M. N. G. (1985) Structure of the calcium regulatory muscle protein troponin-C at 2.8 Å resolution, *Nature 313*, 653−659.
5. Sundaralingam, M., Bergstrom, R., Strasburg, G., Rao, S. T., Roychowdhury, P., Greaser, M., and Wang, B. C. (1985) Molecular structure of troponin C from chicken skeletal muscle at 3 Å resolution, *Science 227*, 945−948.
6. Gagné, S. M., Tsuda, S., Li, M. X., Smillie, L. B., and Sykes, B. D. (1995) Structure of the troponin C regulatory domains in the apo and calcium-saturated state, *Nat. Struct. Biol. 2*, 784−789.
7. Van Eerd, J. P., and Takahashi, K. (1975) The amino acid sequence of bovine cardiac troponin-C: Comparison with rabbit skeletal troponin-C, *Biochem. Biophys. Res. Commun. 64*, 122−127.
8. Li, M. X., Spyracopoulos, L., and Sykes, B. D. (1999) Binding of cardiac troponin-$I_{147-163}$ induces a structural opening in human cardiac troponin-C, *Biochemistry 38*, 8289−8298.
9. Dong, W.-J., Xing, J., Villain, M., Hellinger, M., Robinson, J. M., Chandra, M., Solaro, R. J., Umeda, P. K., and Cheung, H. C. (1999) Conformation of the regulatory domain of cardiac muscle troponin C in its complex with cardiac troponin I, *J. Biol. Chem. 274*, 31382−31390.
10. Takeda, S., Yamashita, A., Maeda, K., and Maeda, Y. (2003) Structure of the core domain of human cardiac troponin in the Ca^{2+}-saturated form, *Nature 424*, 35−41.
11. Spyracopoulos, L., Li, M. X., Sia, S. K., Gagné, S. M., Chandra, M., Solaro, R. J., and Sykes, B. D. (1997) Calcium-induced structural transition in the regulatory domain of human cardiac troponin C, *Biochemistry 36*, 12138−12146.
12. Rabenstein, M. D., and Shin, Y. K. (1995) Determination of the distance between two spin labels attached to a macromolecule, *Proc. Natl. Acad. Sci. U.S.A. 92*, 8239−8243.
13. Nakamura, M., Ueki, S., Hara, H., and Arata, T. (2004) Calcium structural transition of human cardiac troponin C in reconstituted muscle fibers as studied by site-directed spin labeling, *J. Mol. Biol*. (submitted for publication).
14. Dong, W.-J., Wang, C.-K., Gordon, A. M., and Cheung, H. C. (1997) Disparate fluorescence properties of 2-[4′-(iodoacetamido)-anilino]-naphthalene-6-sulfonic acid attached to Cys-84 and Cys-35 of troponin C in cardiac muscle troponin, *Biophys. J. 72*, 850−857.

15. Farah, C. S., Miyamoto, C. A., Ramos, C. H. I., Da Silva, A. C. R., Quaggio, R. B., Fujimori, K., Smillie, L. B., and Reinach, F. C. (1994) Structural and regulatory functions of the NH_2- and COOH-terminal regions of skeletal muscle troponin I, *J. Biol. Chem. 269*, 5230−5240.
16. Moss, R. L. (1992) Ca^{2+} regulation of mechanical properties of striated muscle: Mechanistic studies using extraction and replacement of regulatory proteins, *Circ. Res. 70*, 865−884.
17. Morimoto, S., and Ohtsuki, I. (1987) Ca^{2+}- and Sr^{2+}-sensitivity of the ATPase activity of rabbit skeletal myofibrils: Effect of the complete substitution of troponin C with cardiac troponin C, calmodulin, and parvalbumins, *J. Biochem. 101*, 291−301.
18. Li, H.-C., and Fajer, P. G. (1994) Orientational changes of troponin C associated with thin filament activation, *Biochemistry 33*, 14324−14332.
19. Timofeev, V. P., and Tsetlin, V. I. (1983) Analysis of mobility of protein side chains by spin label technique, *Biophys. Struct. Mech. 10*, 93−108.
20. Xiao, W., and Shin, Y. K. (2000) EPR spectroscopic ruler: The method and its applications, in *Biological Magnetic Resonance. Volume 19: Distance Measurements in Biological Systems by EPR* (Berliner, L. J., Eaton, S. S., and Eaton, G. R., Eds.) Chapter 5, Kluwer, New York.
21. Mchaourab, H. S., Oh, K. J., Fang, C. J., and Hubbel, W. L. (1997) Conformation of T4 lysozyme in solution. Hinge-bending motion and the substrate-induced conformational transition studied by site-directed spin labeling, *Biochemistry 36*, 307−316.
22. Sia, S. K., Li, M. X., Spyracopoulos, L., Gagné, S. M., Liu, W., Putkey, J. A., and Sykes, B. D. (1997) Structure of cardiac muscle troponin C unexpectedly reveals a closed regulatory domain, *J. Biol. Chem. 272*, 18216−18221.
23. Altenbach, C., Oh, K.-J., Trabanino, R. J., Hideg, K., and Hubbell, W. L. (2001) Estimation of inter-residue distances in spin labeling proteins at physiological temperatures: Experimental strategies and practical limitations, *Biochemistry 40*, 15471−15482.
24. Slupsky, C. M., and Sykes, B. D. (1995) NMR solution structure of calcium-saturated skeletal muscle troponin C, *Biochemistry 34*, 15953−15964.
25. Robertson, S. P., Johnson, J. D., Holroyde, M. J., Kranias, E. G., Potter, J. D., and Solaro, R. J. (1982) The effect of troponin I phosphorylation on the Ca^{2+}-binding properties of the Ca^{2+}-regulatory site of bovine cardiac troponin, *J. Biol. Chem. 257*, 260−263.
26. Liao, R., Wang, C. K., and Cheung, H. C. (1994) Coupling of calcium to the interaction of troponin I with troponin C from cardiac muscle, *Biochemistry 33*, 12729−12734.
27. Al Hillawi, E., Bhandari, D. G., Trayer, H. R., and Trayer, I. P. (1995) The effects of phosphorylation of cardiac troponin-I on its interactions with actin and cardiac troponin-C, *Eur. J. Biochem. 228*, 962−970.
28. Heller, W. T., Finley, N. L., Dong, W.-J., Timmins, P., Cheung, H. C., Rosevear, P. R., and Trewhella, J. (2003) Small-angle neutron scattering with contrast variation reveals spatial relationships between the three subunits in the ternary cardiac troponin complex and the effects of troponin I phosphorylation, *Biochemistry 42*, 7790−7800.
29. Ward, D. G., Brewer, S. M., Cornes, M. P., and Trayer, I. P. (2003) A cross-linking study of the N-terminal extension of human cardiac troponin I, *Biochemistry 42*, 10324−10332.
30. Gaponenko, V., Abusamhadneh, E., Abbott, M. B., Finley, N., Gasmi-Seabrook, G., Solaro, R. J., Rance, M., and Rosevear, P. R. (1999) Effects of troponin I phosphorylation on conformational exchange in the regulatory domain of cardiac troponin C, *J. Biol. Chem. 274*, 16681−16684.
31. Finley, N., Abbott, M. B., Abusamhadneh, E., Gaponenko, V., Dong, W.-J., Gasmi-Seabrook, G., Howarth, J. W., Rance, M., Solaro, R. J., Cheung, H. C., and Rosevear, P. R. (1999) NMR analysis of cardiac troponin C-troponin I complexes: Effects of phosphorylation, *FEBS Lett. 453*, 107−112.
32. Abbott, M. B., Dong, W.-J., Dvoretsky, A., DaGue, B., Caprioli, R. M., Cheung, H. C., and Rosevear, P. R. (2001) Modulation of cardiac troponin C-cardiac troponin I regulatory interactions by the amino-terminus of cardiac troponin I, *Biochemistry 40*, 5992−6001.
33. Ward, D. G., Cornes, M. P., and Trayer, I. P. (2002) Structural consequences of cardiac troponin I phosphorylation, *J. Biol. Chem. 277*, 41795−41801.
34. Strynadka, N. C. J., and James, M. N. G. (1989) Crystal structures of the helix-loop-helix calcium-binding proteins, *Annu. Rev. Biochem. 58*, 951−998.
35. Sweeney, H. L., Brito, R. M. M., Rosevear, P. R., and Putkey, J. A. (1990) The low-affinity Ca^{2+}-binding sites in cardiac/slow skeletal muscle troponin C perform distinct functions: Site I alone cannot trigger contraction, *Proc. Natl. Acad. Sci. U.S.A. 87*, 9538−9542.
36. Kraulis, P. J. (1991) MOLSCRIPT: A program to produce both detailed and schematic plots of protein structure, *J. Appl. Crystallogr. 24*, 946−950.
37. Merritt, E. A., and Murphy, E. M. P. (1994) Raster3D Version 2.0: A program for photorealistic molecular graphics, *Acta Crystallogr. D50*, 869−873.

BI048110W